Journal of Anatomy

J. Anat. (2008) **213**, pp202–209 doi: 10.1111/j.1469-7580.2008.00943.x

Identification and characterization of a novel intraepithelial lymphoid tissue in the gills of Atlantic salmon

Erlend Haugarvoll,[1] Inge Bjerkås,[1] Barbara F. Nowak,[2] Ivar Hordvik[3] and Erling O. Koppang[1]

[1]*Section of Anatomy and Pathology, Department of Basic Sciences and Aquatic Medicine, Norwegian School of Veterinary Science, Oslo, Norway*
[2]*School of Aquaculture, University of Tasmania and Aquafin CRC, Launceston, Tasmania, Australia*
[3]*Department of Biology, High Technology Centre, University of Bergen, Norway*

Abstract

In addition to being the respiratory organ in fish, the gills form a barrier against the external milieu. Innate and adaptive immune system components have been detected in the gills, but lymphoid cell accumulations similar to that seen in the mammalian mucosa have not been described. The present investigations revealed cell accumulations on the caudal edge of interbranchial septum at the base of the gill filaments in the Atlantic salmon. Cytokeratin immunohistochemical staining and identification of a basal membrane and desmosome cell junctions by electron microscopy showed that the cell accumulation was located intraepithelially. Major histocompatibility complex (MHC) class II$^+$ cells were detected by immunohistochemistry, and laser capture micro-dissection and subsequent RT-PCR analysis revealed expression of T-cell receptor transcripts in the investigated tissue, suggesting the presence of T cells. The intraepithelial tissue reported here may be a suitable location for immune surveillance of gill infections, as well as a target site for new vaccine approaches and investigations of epithelial immunity. This is the first description of a lymphocyte cell aggregation within a teleostian gill epithelium network, illustrating a phylogenetically early form of leukocyte accumulations in a respiratory organ.

Key words Atlantic salmon; gill; lymphoid organ; mucosa; teleost; thymus development.

Introduction

The gills of modern bony fishes, or teleosts, consist of four paired arches, each containing two rows of posteriolaterally oriented filaments with lamellas covered by respiratory epithelium. The filaments are supported along their proximal third of their length by an interbranchial septum of connective and muscle tissue (Wilson & Laurent, 2002). The respiratory epithelium has multifunctional purposes, which include gas and ion transport, nitrogenous waste excretion and hormone production (Evans et al. 2005). In addition, the mucosa forms the barrier between the organism and the external environment. Fish infectious agents readily spread in the water, and the thin respiratory epithelium of the gills represents an obvious entry for pathogens. For instance, infectious salmon anaemia (ISA) virus infection is believed to be established first in the gills before spreading to other organs (Rimstad & Mjaaland, 2002).

The mammalian intestinal mucosa contains physical barriers and can in addition respond with innate and adaptive immune reactions against invaders (Sansonetti, 2004). The gills form, just like the gut, mucous surfaces designed for selective transport, and harbour mechanisms to avoid infections. Several studies have shown the presence of a highly developed and active immune system. The physical barrier of the fish gills consists of the gill epithelium, a glycocalyx layer and the mucus layer (Powell et al. 1994). Indications of innate and specific immune responses have been suggested by identification of Mx, Toll-like receptor 9 and T-cell receptor (TCR) transcripts (Jensen et al. 2002; Takano et al. 2004, 2007). Koppang et al. (1998a,b) found that the level of major histocompatibility complex (MHC) transcripts in the gills was relatively high compared to the lymphoid pronephros and spleen and that the expression could further be induced following intraperitoneal vaccination. Ohta et al. (2004) cloned and sequenced homologues of the dendritic cell marker CD83 in shark and trout, demonstrating relatively high expression of such transcripts in the gills by Northern blotting.

Correspondence
Dr Erling Olaf Koppang, Section of Anatomy and Pathology, Department of Basic Sciences and Aquatic Medicine, Norwegian School of Veterinary Science, Ullevålsveien 72, PO Box 8146 Dep., 0033 Oslo, Norway. T: +47 22 96 4546; F: +47 22 964764. E: erling.o.koppang@veths.no

Accepted for publication *18 March 2008*

In mammals, the mucosal surfaces harbour aggregations of organized lymphoid cells, i.e. the Peyer's patches of the intestines and tonsils in the pharynx. The localization, architecture and arrangement of these immune tissues are of fundamental importance to determine their function and significance (Mowat, 2003; Pabst et al. 2004). Several studies have investigated the uptake of antigens and the presence of lymphoid cells in the gill epithelium, but no discrete aggregations of such cells or the existence of a lymphoid organ has been described (Ototake et al. 1996; Wilson & Laurent, 2002; Evans et al. 2005).

As the first-line encounter towards antigens, the epithelium of the gills and intestines are important locations for immune reactions. It is therefore likely that these sites should display the first phylogenetic signs of immune cell compartmentalization. Cartilaginous fish and teleosts are among the earliest vertebrate groups to have developed an adaptive immune system comparable to that of mammals (Zapata & Amemiya, 2000). The thymus occurs in all jawed vertebrates, and in mammals, the endodermal primordium of the tonsils and thymus forms from the wall of the second and third pharyngeal pouch, respectively (Sadler, 1995). The thymus in teleosts usually develops from the second to fourth pharyngeal pouches, which are located between the branchial arches (Bowden et al. 2005). The phylogenetic origin of the thymus is not known, but a connection to the mucosa-associated lymphoid tissue has been suggested (Matsunaga & Rahman, 2001). In this model, the primordial thymus develops from integration of intraepithelial leukocytes into an epithelial network, which further may support a high T-cell proliferation. Recently, there has been some attention attracted to the morphological plasticity of thymus construction both in fish and mammals. The thymus is reported to consist of more than one pair of organs in the teleost *Sicyases anguineus*, with one set located near the gill epithelium (Bowden et al. 2005). Further, an ectopic thymus-like tissue was recently discovered in mouse (Terszowski et al. 2006), demonstrating that the arrangement even in mammals is not as rigid as previously assumed.

In a previous study, the use of a polyclonal antibody raised against recombinant MHC class II β chain revealed immunoreactive gill epithelium cells in salmon (Koppang et al. 2003). However, during further investigations it became apparent that lymphoid-like tissue aggregates observed at the base of the gill filaments were highly immunoreactive. When gills are sectioned for histological analysis, they are normally mounted sagitally. We decided to investigate them also in transversal sections through the gill arch. The objectives of the present study were to examine the localization of the lymphoid-like tissue and to investigate the possible presence of aggregates of lymphoid cells.

Materials and methods

Fish

Ten un-vaccinated sea-transferred Atlantic salmon individuals (mean weight 2.63 kg) cultured at Ewos Research Station, Lønningdal, Os, Norway, and four un-vaccinated juveniles 6 months post hatching and two un-vaccinated sea-transferred salmons obtained at Solbergstrand Research Station, Norwegian Institute for Water Research, Drøbak, Norway, were investigated. Thymuses were collected from two un-vaccinated sea-transferred salmons (Ewos Research station). Sea-transferred fish were kept in indoor tanks, receiving water from 70 m depth, and juvenile fish in tanks received treated pathogen-free fresh-water. Histological examination of the gills and other organs revealed no signs of infection. No mortality was recorded in the investigated groups. All fish were euthanized according to regulations for fish in aquaculture issued by the Norwegian Directorate of Fisheries (Forskrift om drift av akvakulturanlegg. § 28. Avlivning av fisk).

Histological examination

Samples from the first gill arch, the head of the four juveniles and the thymus were fixed in 10% neutral buffered formalin for 24 h and decalcinated in 10% formic acid. In one fish, all gill arches were sampled. The gills were prepared for transverse and longitudinal sectioning and the heads for horizontal sectioning at the level of the middle portion of the holobranches, then embedded in paraffin, cut in 4-μm sections and mounted on glass slides. The tissue sections were de-waxed in xylene and rehydrated in graded ethanol baths and stained with hematoxylin and eosin (HE) (Bancroft & Gamble, 2002).

Immunohistochemistry

For detection of MHC class II molecules, the polyclonal antiserum Ø127 (diluted 1 : 1000) raised against a recombinant protein of the salmon MCH class II β chain was used (Koppang et al. 2003). The staining procedure described below was also performed using the following antibodies: Rabbit pAb K555, detecting salmon IgM (1 : 200) (a kind gift from K. Falk, National Veterinary Institute, Oslo, Norway), mAb PC10, identifying proliferating cell nuclear antigen (PCNA) (α-PCNA, No. M0879; Dako, Glostrup, Denmark) (1 : 150), and an mAb AE1/AE3, recognizing mouse cytokeratin (No. 18-0132, Zymed® Laboratories, San Francisco, CA, USA) (1 : 100).

Paraffin sections of 4 μm were cut and mounted on positively charged glass slides (Superfrost® plus, Mentzel, Braunschweig, Germany), incubated at 37 °C for at least 24 h before de-waxing and rehydration. Demasking was achieved by autoclaving in 0.01 M citrate buffer, pH 6.0, at 120 °C for 15 min, cooled to room temperature and then transferred to phosphate-buffered saline (PBS). To inhibit endogenous peroxidase, the sections were treated with phenyl hydrazine (0.05%; Fluka, Buchs, Switzerland) for 40 min at 37 °C.

The following immunostaining was performed in an Autostainer 360 (Lab Vision Corporation, Fremont, CA, USA). To prevent non-specific binding, sections were incubated for 20 min with 5% bovine serum albumin (BSA) in Tris-buffered saline containing normal goat serum diluted 1 : 50. The blocking solution was removed and the sections were incubated with the primary antibody for 60 min. Labeled cells were visualized by an indirect

immunoperoxidase method (EnVision® System, Peroxidase, No. K4009; Dako).

The secondary antibody, horseradish peroxidase-labeled polymer conjugated to goat anti-rabbit (anti-mouse for the monoclonal antibody, No. K4005) Ig, was incubated for 30 min and peroxidase activity was detected following 15 min incubation with the 3-amino-9-ethylcarbazole provided with the EnVision® System kit. The sections were washed twice with PBS for 5 min between each step. The sections were counterstained with hematoxylin for 1 min and mounted with poly-vinyl alcohol mounting media (Ullevål Apotek, Oslo, Norway) before light microscopy examination. Negative controls were performed using 1% BSA. Pig intestine was used as positive control of cytokeratin.

Electron microscopy examination

Transmission electron microscopy (TEM)

Transversally dissected samples of the caudal side of the interbranchial septum between the hemibranches were fixed on ice in 3% glutaraldehyde (GAH) in 0.1 M cacodylate buffer, pH 7.4, post-fixed in 2% OsO_4 and 1.5% $K_3Fe(CN)_6$ in 0.1 M cacodylate buffer, pH 7.2, and then stained *en bloc* with 1.5% uranylacetate before dehydration. Semi-thin (1 μm) sections were cut, mounted on glass slides and stained with toluidine blue. Ultrathin sections of LX 112 Resin (Ladd Research Industries, Williston, VT, USA) embedded tissue samples were post-stained with uranyl acetate and lead citrate and examined in a Philips 208S transmission electron microscope (Eindhoven, The Netherlands).

Scanning electron microscopy (SEM)

Samples of the gill filaments including the interbranchial septum were fixed as described above for TEM and dehydrated in increasing ethanol concentrations, freeze fractured in $N_{(l)}$ chilled ethanol, critical point dried and coated with gold before SEM investigation. Finally, specimens were investigated in a Phillips XL 300 ESEM (Eindhoven, The Netherlands) environmental SEM.

Laser-capture micro-dissection and RT-PCR

Transversal cryo-sections of two gill arches, 7 μm in thickness, were cut with a cryostat and mounted on special membrane slides for laser micro-dissection (No. 50103, Molecular Machines and Industries, Zürich – Glattbrugg, Switzerland). The sections were stained with RNase-free hematoxylin, air-dried and stored at –80 °C until use. Subsequently, the sections were air-dried at room temperature for 2 h and a representative centrally located part of the cell accumulation was laser-capture micro-dissected with the SLμCut micro-dissection system (Molecular Machines and Industries). One to three successive sections, all with an area ranging between 0.05 and 0.19 mm^2, were cut and collected in separate tubes. At least three parallel tubes were prepared for comparison. For T-cell negative controls, cDNA from the salmon macrophage-like SHK-1 cell line was used in addition to water, substituting the cDNA solution.

RNA extraction

Total RNA was isolated from the laser-captured material by using an RNeasy® Micro kit (50) (Qiagen, Hilden, Germany). The kit is designed for isolation of total RNA from minute amounts of frozen, micro-dissected animal tissue. The isolation was performed according to the manufacturer's protocol, including the carrier RNA step for very small samples. The volume of the total RNA solution was 12 μL.

Reverse transcriptase (RT) reaction

Reverse transcription of the 12 μL total RNA solution was performed using Sensiscript® RT kit (Qiagen) according to the producer's instructions. This kit is designed for highly sensitive reverse transcription with small amounts of RNA.

Real-time PCR

MHC class II, TCR and eukaryotic elongation factor 1A (EF1A) primers and amplicon detection probes used for the real-time RT-PCR are described in Table 1. Aliquots of 2 μL of the cDNA solutions from each tissue extraction were used in the real-time experiments with the TaqMan® Probe-based Detection system (Applied Biosystems, Foster City, CA, USA) and the IQ supermix (Bio-Rad Laboratories, Hercules, CA, USA) with a final volume of 20 μL PCR solution, primer concentration 900 nM and probe concentration 200 nM. The real-time experiments were performed in a Chromo 4 (Bio-Rad Laboratories) real-time detection system, with the following settings: 2 min at 50 °C, 15 min at 95 °C, 50 cycles of 15 s at 95 °C, 50 s at 60 °C.

Results

Light and electron microscopy

Light microscopic investigations of transversally sectioned gill arches from the sea-transferred salmon displayed a triangular cell mass on the caudal side of each of the interbranchial septa, and at each side it extended along the epithelium of the gill filaments (Figs 1, 2). SEM analysis revealed that this cell accumulation formed a continuous ridge along the caudal surface of the gill arches in the slit between the hemibranches (Figs 3, 4). Light-microscopically, the most superficial layer consisted of regular gill epithelial cells and numerous goblet cells, and the main cell mass

Table 1 TaqMan assays used to detect gene expression. The MHC class II assay was designed for the present study. The TCR and EF1A assays have been described in previous studies (Moore et al. 2005; Olsvik et al. 2005)

Gene	Forward primer	Reverse primer	TaqMan probe
MHC class II	CTCACTGAGCCCATGGTGTAT	GAGTCCTGCCAAGGCTAAGATG	CTGGGACCCGTCCCTG
TCRα	GACAGCTACTACAGCCAGGTT	CAGAATGGTCAGGGATAGGAAGTT	ACACAGATGCAAAGATC
EF1A	CCCCTCCAGGACGTTTACAAA	CACACGGCCCACAGGTACA	ATCGGTGGTATTGGAAC

contained many lymphocyte-like cells (Figs 5, 6). The most basal cells formed a continuous palisade-like pattern (Fig. 5), in which mitotic figures were regularly observed. Blood vessels were not found in the cell accumulation, but a vascular connective tissue with many capillaries, being continuous with the lamina propria of the gill mucosa, was bordering beneath the basal cells (Fig. 7). In the juveniles, similar tissues were observed on the caudal rim of the interbranchial septum (data not shown).

TEM displayed numerous cells of epithelial type with abundant desmosomes and intracytoplasmic intermediate filaments (Fig. 6). From the base to the apex of the cell accumulation, the epithelial cells formed a trabecular network surrounding groups of lymphocyte-like cells (Fig. 6). The epithelial cell processes were readily interdigitating and displayed numerous desmosomes, whereas the cells of the lymphocyte type had a small cytoplasm and showed no clear desmosomes or intermediate filaments (Fig. 6). The epithelial cells formed a continuous basal layer and were attached to a basal lamina that was continuous with the basal lamina of the gill filament epithelium (Fig. 8). The basal lamina created a border to the underlying vascular connective tissue (Figs 8, 9).

Immunohistochemistry

The antiserum against cytokeratin stained cells in the epithelium along the gill filaments and lamellae and in the accumulations of cells (Fig. 10). In the latter, there was positive staining of numerous trabecular structures, which surrounded small groups of non-reacting cells (Fig. 9). In the thymus sections, the cytokeratin staining displayed a quite similar trabecular pattern (Fig. 11). No staining was observed in the connective tissue.

In PCNA stained sections, positive cells were most numerous in the basal areas of the cell accumulations, but were also dispersed in the gill filament epithelium (Fig. 12). Many of the red PCNA-reacting nuclei displayed a dark granular staining (Fig. 12, insert).

Abundant MHC class II$^+$ cells were detected in the epithelium on the caudal rim of the interbranchial septum and in the epithelium covering the gill filaments (Fig. 13). Immunoreactive cells were dispersed evenly in the investigated tissue, but appeared to be most frequent close to the apical surface.

IgM staining was neither detected in the present cell accumulation nor in the gill epithelium. Blood plasma was IgM$^+$.

Polymerase chain reaction investigations of micro-dissected samples

Six micro-dissected samples (Fig. 14) from the investigated gill tissue were subjected to real time PCR, utilizing TaqMan assays for EF1A, MHC class II and TCR α. Due to small amounts of cDNA in the samples (Ct values between 31 and 35), a more comprehensive study is required to obtain quantitative data. However, a comparison of the present Ct values and raw data from several tissues of Atlantic salmon (Moore et al. 2005; and unpublished results) strongly indicate that the abundance of TCR α transcripts in the investigated tissue is high. No amplification was detected in negative controls.

Discussion

In this study, the gills of sea-transferred salmon were demonstrated to exhibit large intraepithelial cell aggregations at the caudal rim of each of the interbranchial septa. The accumulation of cells displayed a trabecular pattern of cytokeratin positive cells, and had desmosome cell junctions, bordered by a continuous superficial and basal layer of cytokeratin positive cells. The tissue harboured PCNA$^+$ cells and the observation of MHC class II$^+$ cells and expression of TCR in the cell accumulations are all indications of an organized lymphoid tissue. IgM$^+$ cells were not seen intraepithelially. Similar cell accumulations were also observed in investigated juveniles.

Cytokeratin intermediate filaments are characteristic of epithelial tissues, and the cytokeratins exhibit a high degree of homology among vertebrates (Schaffeld & Markl, 2004). In the present investigations, a commercial mouse anti-cytokeratin antibody stained cells of the investigated caudal rim of the intrabranchial septum and in the gill filament epithelium. Electron microscopic studies confirmed intermediate filaments in the epithelium cells and many of them were attached by desmosomes, which also are specific for epithelial tissues (Garrod et al. 2002), and the basal cells shared a common basal lamina with the gill filament epithelium. These findings showed that the cell aggregation was located within the gill epithelium.

PCNA is a highly conserved protein in eukaryotes and is expressed during cell proliferation and repair (Yu & Filipe, 1993; Lee & Gye, 1999; Leung et al. 2005). The protein has long half-life, and a dark granular staining in nucleus may correspond more closely to the S-phase of the cell cycle (Yu & Filipe, 1993). In this study, the mouse anti-PCNA antibody displayed a dark granular staining, and mitotic figures were detected in the basal cell layers. This indicated substantial cell proliferation in the investigated gill epithelium and in the basal portions of the filament epithelium. Cell proliferation in the latter has been described previously in fish (Zenker et al. 1987).

In mammalian and fish mucosal membranes, intraepithelial leukocytes mainly consist of T cells and some macrophages (Picchietti et al. 1997; Zapata & Amemiya, 2000; Huttenhuis et al. 2006; Romano et al. 2007). In addition, dendritic cells are able to send cytoplasmic protrusions through the epithelium towards the intestinal lumen for antigen recognition and sampling (Rescigno et al. 2001). To further investigate the nature of the cells in the present tissue, we applied available leukocyte markers.

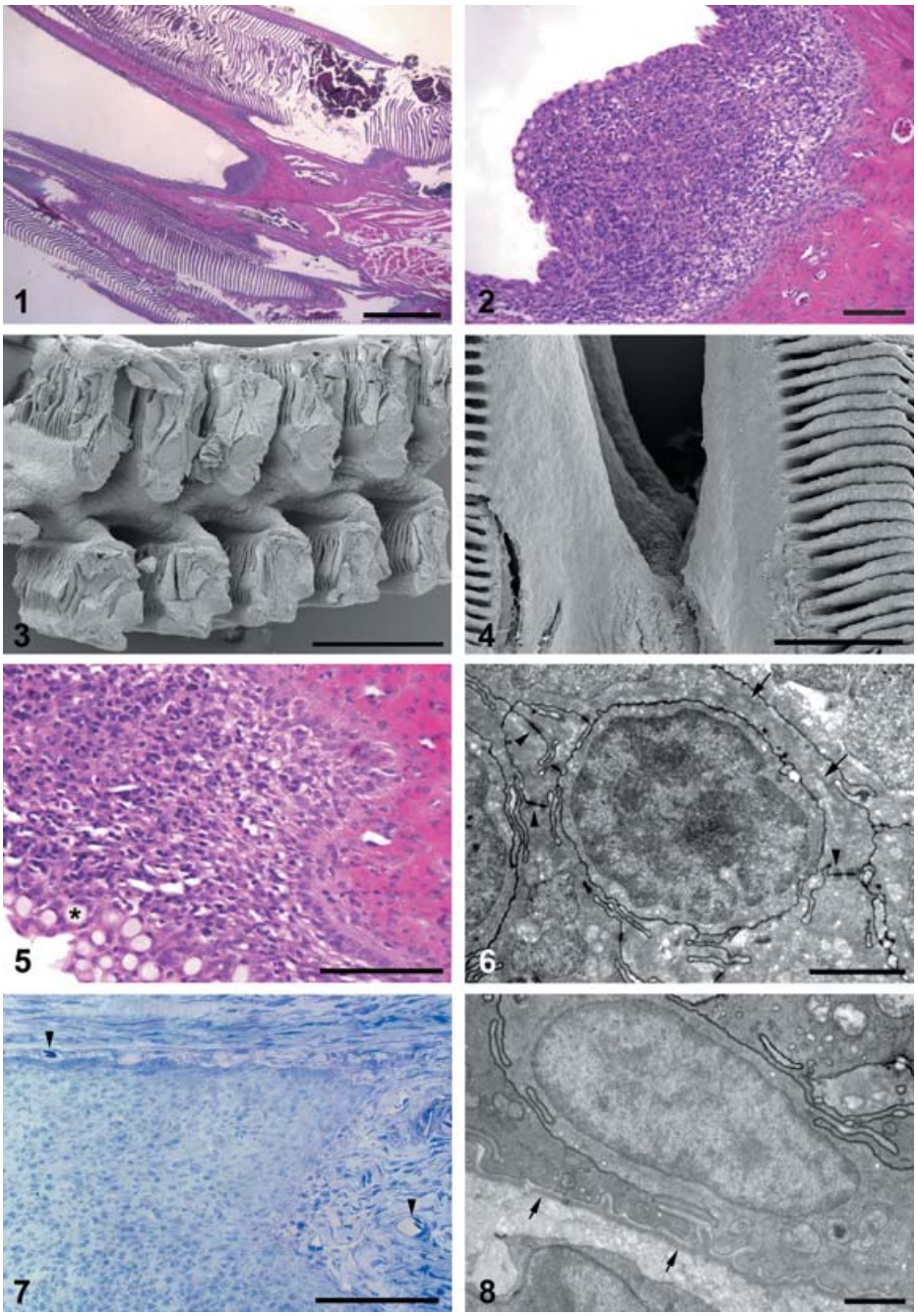

Figs 1 and 2 Micrograph of a transversely sectioned gill arch. The cell accumulation on the caudal edge of an interbranchial septum is seen in the slit between the gill filaments and it is extended along the epithelium of the gill filaments. The apparently thickened areas of the gill lamellae seen at the upper left in Fig. 1 represent either areas with dilated capillaries or tilted regions cut at an angle. HE. Scale bars 1 mm, 100 μm.
Figs 3 and 4 Scanning electron micrographs of the posteriolateral surface of a gill arch. A continuous ridge is displayed in the slit between the filaments. Scale bars 200 μm, 500 μm.
Fig. 5 A close-up micrograph of the investigated cell accumulation. The basal cells display a palisade-like pattern and small cells with dark nucleus and thin cytoplasm are observed in the parenchyma. Goblet cells are seen at the mucosal surface (asterisk). HE. Scale bar 100 μm.
Fig. 6 Transmission electron micrograph of a lymphocyte-like cell in the investigated cell accumulation. Desmosome cell junctions are seen connecting the surrounding epithelial cells (arrowheads), and intermediate filaments are observed inside one of them (arrows). Scale bar 2 μm.
Fig. 7 A micrograph showing the blood vessel network of the adjacent connective tissue (lamina propria). Arrowheads indicate blood vessels with erythrocytes. Toluidine blue. Scale bar 100 μm.
Fig. 8 Transmission electron micrograph of the basal lamina in the investigated cell accumulation. The basal lamina (arrows) is seen below the epithelium. Scale bar 1 μm.

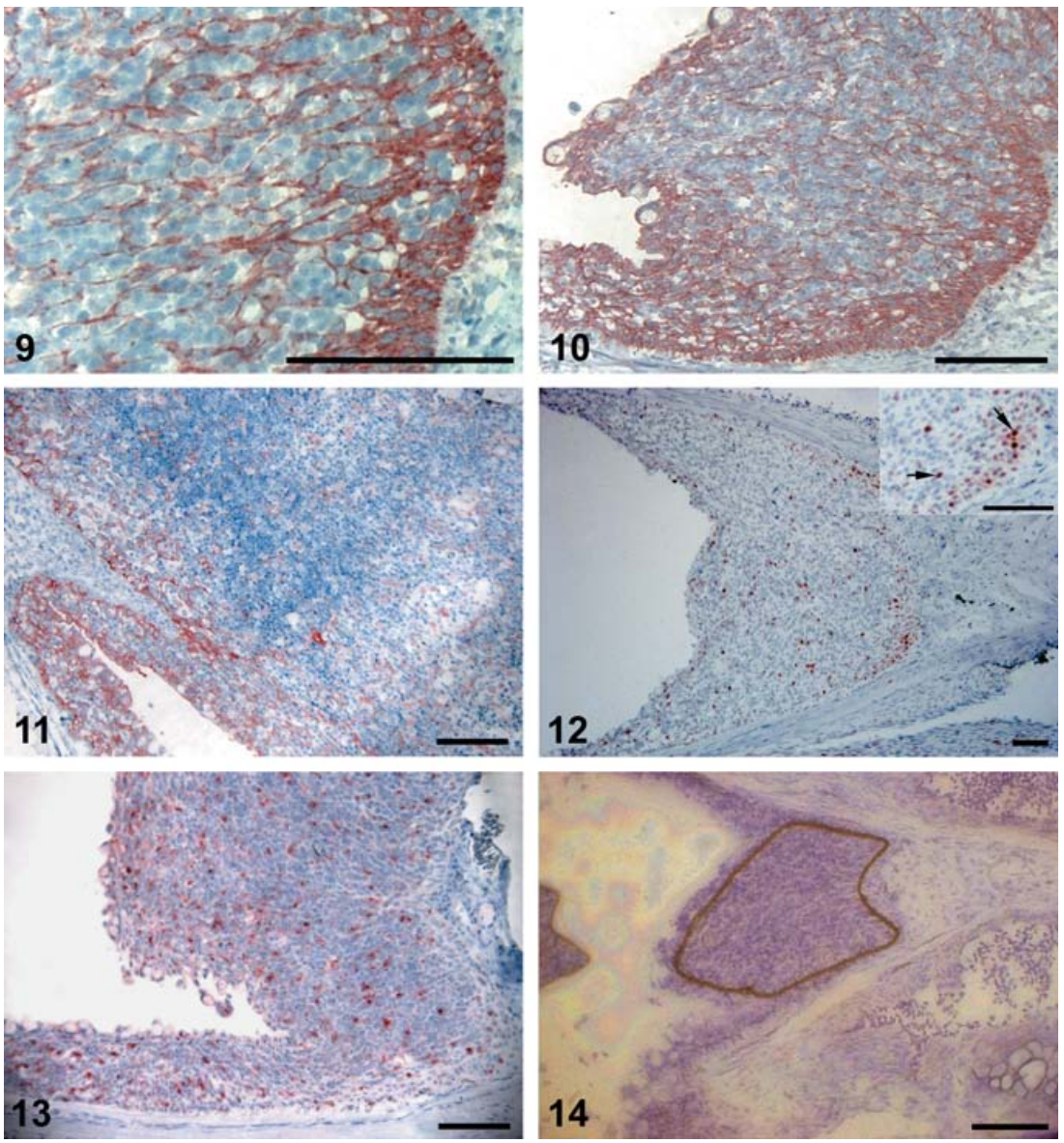

Fig. 9 Immunohistochemical detection of cytokeratin in the investigated cell accumulation. Small groups of cells are enveloped by cytokeratin-stained cells. The basal layer forms a distinct border to the underlying connective tissue. Scale bar 100 μm.
Fig. 10 Immunohistochemical detection of cytokeratin in the investigated cell accumulation. The basal layer is especially strongly stained, sending a trabecular network towards the apex. Cells at the surface are positively stained and goblet cells are seen. Strong staining for cytokeratin was also detected in the epithelium along the gill filament. Scale bar 100 μm.
Fig. 11 Immunohistochemical detection of cytokeratin in the thymus. Cytokeratin stained trabeculae are extending into the parenchyma. Scale bar 100 μm.
Fig. 12 PCNA staining for detection of cell proliferation. PCNA positive cells are most frequent in the basal regions, whereas only scattered cells are stained in other areas. The inset shows an enlarged area of a basal region, displaying granular staining of nuclei (arrows). Scale bars 100 μm.
Fig. 13 Immunohistochemical detection of MHC class II in the investigated cell accumulation. Abundant MHC class II$^+$ cells are dispersed in the cell accumulation and in the epithelium covering the trailing edge of the gill filament. Scale bar 100 μm.
Fig. 14 A micrograph of a laser micro-dissected cryo-section. A representative part of the cell accumulation was laser micro-dissected (brown line) and attached to the cap of a plastic tube ready for collection. Toluidine blue. Scale bar 100 μm.

The thymus of salmonids harbours MHC class II$^+$ cells in a fashion similar to that of mammals, and TCR transcripts are expressed (Koppang et al. 2003; Fischer et al. 2005). The selection and development of T cells is highly dependent on an intimate connection with the network of the reticular epithelial cells and their expression of MHC molecules (Matsunaga & Rahman, 2001). The observation of an epithelial cell network in the gill structure, which also harboured abundant MHC class II$^+$ cells distributed in a similar fashion as previously observed in the salmon

thymus (Koppang et al. 2003), strongly suggests functional analogies between these tissues. MHC class II expression may be observed in cells of the leukocyte lineage including dendritic cells, macrophages, B cells and T cells, but epithelial cells may also be positive (Glimcher & Kara, 1992).

Further, IgM^+ cells were not detected intraepithelially. The information of IgM^+ cells in the gill mucosa of different fish species is conflicting, and there is evidence that the gills harbour a local population of IgM-producing cells in some fish species (Dos Santos et al. 2001). IgM^+ cells have been detected in the gill filament epithelium of halibut (*Hippoglossus hippoglossus*) and in spotted wolffish (*Anarhichas minor* Olafsen) (Grøntvedt & Espelid, 2003). In cod, IgM^+ cells were detected in the connective tissue and in blood plasma, which were similar to the findings of the present study (Schrøder et al. 1998). These data indicate species-specific distributional differences of IgM^+ cells in the gill mucosa. Further, the gill mucosa of salmon may be supplied by IgM from cells at other locations than in the epithelium. It is also possible, but not likely, that the mucosal IgM is different from serum IgM, as reported in carp (Rombout et al. 1993), and was not detected by the polyclonal antibody used in this study.

TCR mRNA expression was detected in the intraepithelial micro-dissected material and many lymphocyte-like cells were observed in the tissue sections. In trout intestine, intraepithelial lymphocytes mainly consist of IgM^- cells expressing TCRs (Bernard et al. 2006). TCR molecules are restricted to T cells in mammals and TCR α-positive cells have been found in gill epithelium of zebrafish embryos (Danilova et al. 2004). Intraepithelial lymphocytes seem to proliferate in the gut of mammals (Ishikawa et al. 2007) and cell proliferation was observed in the investigated epithelium in this study. It is tempting to suggest such an analogy between the mammalian intestinal and the teleost respiratory mucosal surfaces; however, the nature of the cells in the latter could not be determined. Given these considerations, the results in this study strongly indicate T-cell presence in the investigated intraepithelial tissue.

The trabecular network visualized by cytokeratin staining in the present study shows similarities to the epithelial trabecula observed in the thymus. Such an epithelial network may be a structure providing a basis for the evolution of a T-cell-rich thymus (Matsunaga & Rahman, 2001). In addition, the presence of MHC $class\ II^+$ cells and expression of TCR in the cell accumulations are further indications of a lymphoid organ.

In fish, the degree of involution of the thymus is described to vary in different teleost species (Bowden et al. 2005). The investigated intraepithelial tissue was present in both juveniles and in adult salmon, indicating that a T-cell-rich tissue persists here throughout the salmon adult life.

The tonsils are lymphoid organs located in the pharynx of mammals and, similar to the thymus, evolve from the pharyngeal pouches. The germinal centres of the tonsils contain both B and T cells, but IgM^+ cells were not detected in the intraepithelial cell aggregations in this study.

Morphological investigations of the teleost immune system are severely hampered by the lack of leukocyte cell markers (Koppang et al. 2007). Currently, our laboratory is collaborating with others to establish useful salmonid T-cell markers. Such markers would have been of significant help in the current study.

The present article describes novel intraepithelial lymphoid cell aggregations in the salmon gills. These aggregations are most likely part of the gill mucosal immune system, illustrating a phylogenetic early differentiation and compartmentalization of a respiratory organ immune apparatus. Our discovery can provide new information related to thymus phylogeny and the development of lymphoid tissues and mucosal immunity. From a practical point of view, the results may be useful in relation to studies of gill infections and the development, administration and uptake of new mucosal vaccines applicable for large amounts of fish.

Acknowledgements

Mr Steinar Stølen, Faculty of Dentistry, University of Oslo, Mrs Hege Ellingsen and Mr Qirong Huang, Department of Basic Sciences and Aquatic Medicine, are thanked for meticulous technical assistance. This project was funded by grants from the Norwegian School of Veterinary Science; Lingalaks AS, Strandebarm and the Norwegian Research Council FUGE SalEx programme, Oslo, Norway.

References

Bancroft JB, Gamble M (2002) *Theory and Practice of Histological Techniques*, 5th edn. London: Churchill Livingstone.

Bernard D, Six A, Rigottier-Gois L, et al. (2006) Phenotypic and functional similarity of gut intraepithelial and systemic T cells in a teleost fish. *J Immunol* **176**, 3942–3949.

Bowden TJ, Cook P, Rombout JHWM (2005) Development and function of the thymus in teleosts. *Fish Shellfish Immunol* **19**, 413–427.

Danilova N, Hohman VS, Sacher F, et al. (2004) T cells and the thymus in developing zebrafish. *Dev Comp Immunol* **28**, 755–767.

Dos Santos NMS, Taverne-Thiele JJ, Barnes AC, et al. (2001) The gill is a major organ for antibody secreting cell production following direct immersion of sea bass (*Dicentrarchus labrax*, L.) in a *Photobacterium damselae* ssp. *piscicida* bacterin: an ontogenetic study. *Fish Shellfish Immunol* **11**, 65–74.

Evans DH, Piermarini PM, Choe KP (2005) The multifunctional fish gill: dominant site of gas exchange, osmoregulation, acid-base regulation, and excretion of nitrogenous waste. *Physiol Rev* **85**, 97–177.

Fischer U, Dijkstra JM, Köllner B, et al. (2005) The ontogeny of MHC class I expression in rainbow trout (*Oncorhynchus mykiss*). *Fish Shellfish Immunol* **18**, 49–60.

Garrod DR, Merritt AJ, Nie Z (2002) Desmosomal cadherins. *Curr Opin Cell Biol* **14**, 537–545.

Glimcher LH, Kara CJ (1992) Sequences and factors: a guide to MHC class-II transcription. *Annu Rev Immunol* **10**, 13–49.

Grøntvedt RN, Espelid S (2003) Immunoglobulin producing cells in the spotted wolffish (*Anarhichas minor* Olafsen): localization in adults and during juvenile development. *Dev Comp Immunol* **27**, 569–578.

Huttenhuis H, Romano N, van Oosterhoud C, et al. (2006) The ontogeny of mucosal immune cells in common carp (*Cyprinus carpio* L.). *Anat Embryol* **211**, 19–29.

Ishikawa H, Naito T, Iwanaga T, et al. (2007) Curriculum vitae of intestinal intraepithelial T cells: their developmental and behavioral characteristics. *Immunol Rev* **215**, 154–165.

Jensen I, Albuquerque A, Sommer AI, Robertsen B (2002) Effect of poly I : C on the expression of Mx proteins and resistance against infection by infectious salmon anaemia virus in Atlantic salmon. *Fish Shellfish Immunol* **13**, 311–326.

Koppang EO, Lundin M, Press CM, Rønningen K, Lie Ø (1998a) Differing levels of Mhc class IIβ chain expression in a range of tissues from vaccinated and non-vaccinated Atlantic salmon (*Salmo salar* L.). *Fish Shellfish Immunol* **8**, 183–196.

Koppang EO, Press CM, Rønningen K, Lie Ø (1998b) Expression of Mhc class I mRNA in tissues from vaccinated and non-vaccinated Atlantic salmon (*Salmo salar* L.). *Fish Shellfish Immunol* **8**, 577–587.

Koppang EO, Hordvik I, Bjerkås I, et al. (2003) Production of rabbit antisera against recombinant MHC class IIβ chain and identification of immunoreactive cells in Atlantic salmon (*Salmo salar*). *Fish Shellfish Immunol* **14**, 115–132.

Koppang EO, Fischer U, Satoh M, Jirillo E (2007) Inflammation in fish as seen from a morphological point of view with special reference to the vascular compartment. *Curr Pharm Des* **13**, 3649–3655.

Lee JS, Gye MC (1999) Zebrafish *Danio rerio* proliferating cell nuclear antigen (PCNA): cloning and characterization. *Fish Sci* **65**, 955–958.

Leung AYH, Leung JCK, Chan LYY, et al. (2005) Proliferating cell nuclear antigen (PCNA) as a proliferative marker during embryonic and adult zebrafish hematopoiesis. *Histochem Cell Biol* **124**, 105–111.

Matsunaga T, Rahman A (2001) In search of the origin of the thymus: the thymus and GALT may be evolutionarily related. *Scand J Immunol* **53**, 1–6.

Moore LJ, Somamoto T, Lie KK, Dijkstra JM, Hordvik I (2005) Characterisation of salmon and trout CD8α and CD8β. *Mol Immunol* **42**, 1225–1234.

Mowat AM (2003) Anatomical basis of tolerance and immunity to intestinal antigens. *Nat Rev Immunol* **3**, 331–341.

Ohta Y, Landis E, Boulay T, et al. (2004) Homologs of CD83 from Elasmobranch and teleost fish. *J Immunol* **173**, 4553–4560.

Olsvik PA, Lie KK, Jordal AE, Nilsen TO, Hordvik I (2005) Evaluation of potential reference genes in real-time RT-PCR studies of Atlantic salmon. *BMC Mol Biol* **6**, 21.

Ototake M, Iwama GK, Nakanishi T (1996) The uptake of bovine serum albumine by the skin of bath-immunised rainbow trout *Oncorhynchus mykiss*. *Fish Shellfish Immunol* **6**, 321–333.

Pabst O, Herbrand H, Bernhardt G, Forster R (2004) Elucidating the functional anatomy of secondary lymphoid organs. *Curr Opin Immunol* **16**, 394–399.

Picchietti S, Terribili FR, Mastrolia L, Scapigliati G, Abelli L (1997) Expression of lymphocyte antigenic determinants in developing gut-associated lymphoid tissue of the sea bass *Dicentrarchus labrax* (L.). *Anat Embryol* **196**, 457–463.

Powell MD, Speare DJ, Wright GM (1994) Comparative ultrastructural morphology of lamellar epithelial, chloride and mucus cell glycocalyx of the rainbow trout (*Oncorhynchus mykiss*) gill. *J Fish Biol* **44**, 725–730.

Rescigno M, Urbano M, Valzasina B, et al. (2001) Dendritic cells express tight junction proteins and penetrate gut epithelial monolayers to sample bacteria. *Nat Immunol* **2**, 361–367.

Rimstad E, Mjaaland S (2002) Infectious salmon anaemia virus. An orthomyxovirus causing an emerging infection in Atlantic salmon. *APMIS* **110**, 273–282.

Romano N, Rossi F, Abelli L, et al. (2007) Majority of TcRβ + T-lymphocytes located in thymus and midgut of the bony fish, *Dicentrarchus labrax* (L.). *Cell Tissue Res* **329**, 479–489.

Rombout JHWM, Taverne N, van de Kamp M, Taverne-Thiele AJ (1993) Differences in mucus and serum immunoglobulin of carp (*Cyprinus carpio* L.). *Dev Comp Immunol* **17**, 309–317.

Sadler TW (1995) Head and neck. In *Langman's Medical Embryology*, 7th edn. (ed. Sadler TW), pp. 312–346. Baltimore: Williams & Wilkins.

Sansonetti PJ (2004) War and peace at mucosal surfaces. *Nat Rev Immunol* **4**, 953–964.

Schaffeld M, Markl J (2004) Fish keratins. *Methods Cell Biol* **78**, 627–671.

Schrøder MB, Flano E, Pilström L, Jørgensen TØ (1998) Localisation of Ig heavy chain mRNA positive cells in Atlantic cod (*Gadus morhua* L.) tissues; identified by *in situ* hybridisation. *Fish Shellfish Immunol* **8**, 565–576.

Takano T, Iwahori A, Hirono I, Aoki T (2004) Development of a DNA vaccine against hirame rhabdovirus and analysis of the expression of immune-related genes after vaccination. *Fish Shellfish Immunol* **17**, 367–374.

Takano T, Kondo H, Hirono I, et al. (2007) Molecular cloning and characterization of Toll-like receptor 9 in Japanese flounder, *Paralichthys olivaceus*. *Mol Immunol* **44**, 1845–1853.

Terszowski G, Muller SM, Bleul CC, et al. (2006) Evidence for a functional second thymus in mice. *Science* **312**, 284–287.

Wilson JM, Laurent P (2002) Fish gill morphology: inside out. *J Exp Zool* **293**, 192–213.

Yu CCW, Filipe IM (1993) Update on proliferation-associated antibodies applicable to formalin-fixed paraffin-embedded tissue and their clinical application. *Histochem J* **25**, 843–853.

Zapata A, Amemiya CT (2000) Phylogeny of lower vertebrates and their immunological structures. *Curr Top Microbiol Immunol* **248**, 67–107.

Zenker WG, Ferguson HW, Barker IK, Woodward B (1987) Epithelial and pillar cell replacement in gills of juvenile trout, *Salmo gairdneri* Richardson. *Comp Biochem Physiol A* **86**, 423–428.